

Table 2. Selected geometric parameters (Å, °)

Mo(1)—O(1)	1.70 (3)	Rb(1)—O(5 ^{iv})	2.86 (3)
Mo(1)—O(2)	2.03 (3)	Rb(1)—O(5)	2.86 (3)
Mo(1)—O(3)	2.11 (3)	Rb(1)—O(7)	2.86 (3)
Mo(1)—O(4)	2.09 (3)	Rb(1)—O(7 ^{iv})	2.86 (3)
Mo(1)—O(5)	1.87 (3)	Rb(1)—O(8 ^v)	2.76 (3)
Mo(1)—O(6)	2.20 (3)	Rb(1)—O(8 ⁱⁱⁱ)	2.76 (3)
Mo(2)—O(5)	1.85 (3)	Rb(2)—O(1 ⁱⁱ)	3.05 (3)
Mo(2)—O(7)	1.70 (3)	Rb(2)—O(4)	3.05 (3)
Mo(2)—O(8)	2.10 (3)	Rb(2)—O(6)	3.23 (3)
Mo(2)—O(9)	2.04 (3)	Rb(2)—O(7 ^{vi})	3.06 (3)
Mo(2)—O(10)	2.08 (3)	Rb(2)—O(7 ^{vii})	3.10 (3)
Mo(2)—O(11)	2.13 (3)	Rb(2)—O(8 ^{viii})	3.39 (3)
P(1)—O(2 ⁱ)	1.55 (3)	Rb(2)—O(9 ^{viii})	3.23 (3)
P(1)—O(4 ⁱⁱ)	1.54 (3)	Rb(2)—O(10 ^{vi})	3.04 (3)
P(1)—O(6)	1.53 (3)	Rb(2)—O(11 ^{viii})	2.93 (3)
P(1)—O(11)	1.53 (3)	Rb(3)—O(2 ⁱ)	3.00 (3)
P(2)—O(3)	1.53 (3)	Rb(3)—O(3)	2.89 (3)
P(2)—O(8 ⁱⁱⁱ)	1.54 (3)	Rb(3)—O(3 ^{ix})	2.89 (3)
P(2)—O(9 ⁱ)	1.54 (3)	Rb(3)—O(4)	2.97 (3)
P(2)—O(10)	1.56 (3)	Rb(3)—O(4 ^{ix})	2.88 (3)
Rb(1)—O(1 ^{iv})	2.89 (3)	Rb(3)—O(6)	3.25 (3)
Rb(1)—O(1)	2.89 (3)	Rb(3)—O(6 ⁱ)	3.12 (3)
O(2 ⁱ)—P(1)—O(4 ⁱⁱ)	109 (2)	O(3)—Mo(1)—O(4)	88 (1)
O(2 ⁱ)—P(1)—O(6)	109 (2)	O(3)—Mo(1)—O(5)	84 (1)
O(2 ⁱ)—P(1)—O(11)	112 (2)	O(3)—Mo(1)—O(6)	83 (1)
O(4 ⁱⁱ)—P(1)—O(6)	109 (2)	O(4)—Mo(1)—O(5)	165 (1)
O(4 ⁱⁱ)—P(1)—O(11)	106 (2)	O(4)—Mo(1)—O(6)	81 (1)
O(6)—P(1)—O(11)	112 (2)	O(5)—Mo(1)—O(6)	86 (1)
O(3)—P(2)—O(8 ⁱⁱⁱ)	110 (2)	O(5)—Mo(2)—O(7)	99 (1)
O(3)—P(2)—O(9 ⁱ)	107 (2)	O(5)—Mo(2)—O(8)	171 (1)
O(3)—P(2)—O(10)	115 (2)	O(5)—Mo(2)—O(9)	91 (1)
O(8 ⁱⁱⁱ)—P(2)—O(9 ⁱ)	110 (2)	O(5)—Mo(2)—O(10)	89 (1)
O(8 ⁱⁱⁱ)—P(2)—O(10)	107 (2)	O(5)—Mo(2)—O(11)	88 (1)
O(9 ⁱ)—P(2)—O(10)	108 (2)	O(7)—Mo(2)—O(8)	90 (1)
O(1)—Mo(1)—O(2)	96 (1)	O(7)—Mo(2)—O(9)	102 (1)
O(1)—Mo(1)—O(3)	94 (1)	O(7)—Mo(2)—O(10)	93 (1)
O(1)—Mo(1)—O(4)	92 (1)	O(7)—Mo(2)—O(11)	170 (1)
O(1)—Mo(1)—O(5)	101 (1)	O(8)—Mo(2)—O(9)	88 (1)
O(1)—Mo(1)—O(6)	172 (1)	O(8)—Mo(2)—O(10)	90 (1)
O(2)—Mo(1)—O(3)	170 (1)	O(8)—Mo(2)—O(11)	83 (1)
O(2)—Mo(1)—O(4)	93 (1)	O(9)—Mo(2)—O(10)	165 (1)
O(2)—Mo(1)—O(5)	92 (1)	O(9)—Mo(2)—O(11)	85 (1)
O(2)—Mo(1)—O(6)	87 (1)	O(10)—Mo(2)—O(11)	80 (1)

Symmetry codes: (i) $x, \frac{1}{2} - y, \frac{1}{2} + z$; (ii) $1 - x, \frac{1}{2} + y, \frac{1}{2} - z$; (iii) $-x, y - \frac{1}{2}, \frac{1}{2} - z$; (iv) $-x, -y, -z$; (v) $x, \frac{1}{2} - y, z - \frac{1}{2}$; (vi) $1 + x, y, z$; (vii) $1 + x, \frac{1}{2} - y, \frac{1}{2} + z$; (viii) $1 - x, y - \frac{1}{2}, \frac{1}{2} - z$; (ix) $1 - x, -y, 1 - z$.

Calculations were performed with the *SDP* system (Frenz, 1982) using a MicroVAX II computer. Molecular graphics: *MOLVIEW*.

Lists of structure factors and anisotropic displacement parameters have been deposited with the IUCr (Reference: DU1083). Copies may be obtained through The Managing Editor, International Union of Crystallography, 5 Abbey Square, Chester CH1 2HU, England.

References

- Borel, M. M., Leclaire, A., Grandin, A. & Raveau, B. (1994). *J. Solid State Chem.* **108**, 336–339.
 Borel, M. M., Leclaire, A., Guesdon, A., Grandin, A. & Raveau, B. (1994). *J. Solid State Chem.* In the press.
 Frenz, B. A. (1982). *Enraf-Nonius Structure Determination Package*. College Station, Texas, USA.
 Gueho, C., Borel, M. M., Grandin, A., Leclaire, A. & Raveau, B. (1993). *J. Solid State Chem.* **104**, 202–208.
 Guesdon, A., Borel, M. M., Grandin, A., Leclaire, A. & Raveau, B. (1993). *Acta Cryst.* **C49**, 1877–1879.
 Zachariasen, W. H. (1963). *Acta Cryst.* **16**, 1139–1145.

Acta Cryst. (1994). **C50**, 1854–1857

Thallous Nitrate (III); a Single-Crystal Neutron Study

P. U. M. SASTRY, H. RAJAGOPAL AND A. SEQUIERA

*Solid State Physics Division,
 Bhabha Atomic Research Centre, Trombay,
 Bombay 400085, India*

(Received 26 October 1993; accepted 19 May 1994)

Abstract

The structure of TlNO₃ (III) is refined from single-crystal neutron diffraction data with significantly improved accuracy compared to the reported X-ray structure. Rigid-body thermal-motion analysis indicates that the largest amplitude of libration is about the plane normal to one of the nitrate ions and about an in-plane axis for the other. The maximum librational frequencies for both nitrate groups, however, are about the in-plane axes, and are in close agreement with the values reported from a Raman scattering study.

Comment

TlNO₃ is known to exhibit interesting high-temperature structural phase transitions from the room-temperature orthorhombic phase (III) to a hexagonal phase (II) and then to a cubic phase (I), involving reorientation of the planar nitrate ions (Brown & McLaren, 1962; Fraser, Kennedy & Snow, 1975). However, the structural details of these high-temperature phases have not been reported. In order to understand the mechanism of these transitions, a neutron study of TlNO₃ was initiated. This paper reports the results of a single-crystal neutron study of TlNO₃ (III).

The structural parameters obtained using neutron data, although essentially in agreement with the values obtained from X-ray data (Fraser, Kennedy & Snow, 1975), are far more accurate for all of the atoms with the exception of the Tl atom. As shown in Table 2, there are no significant differences in the atomic coordinates obtained from the neutron study and the X-ray study. Only the values for the x coordinates of the atoms N(2) and O(2) differ by more than their respective e.s.d.'s. A view of the structure is shown in Fig. 1, which shows that the nitrate ions are enclosed within distorted cubes formed by a pseudo-cubic lattice of Tl ions. The edge lengths of each cube range from 3.9 to 4.7 Å. The nitrate ions are oriented such that the planes through the ions are almost normal to one of the cube edges

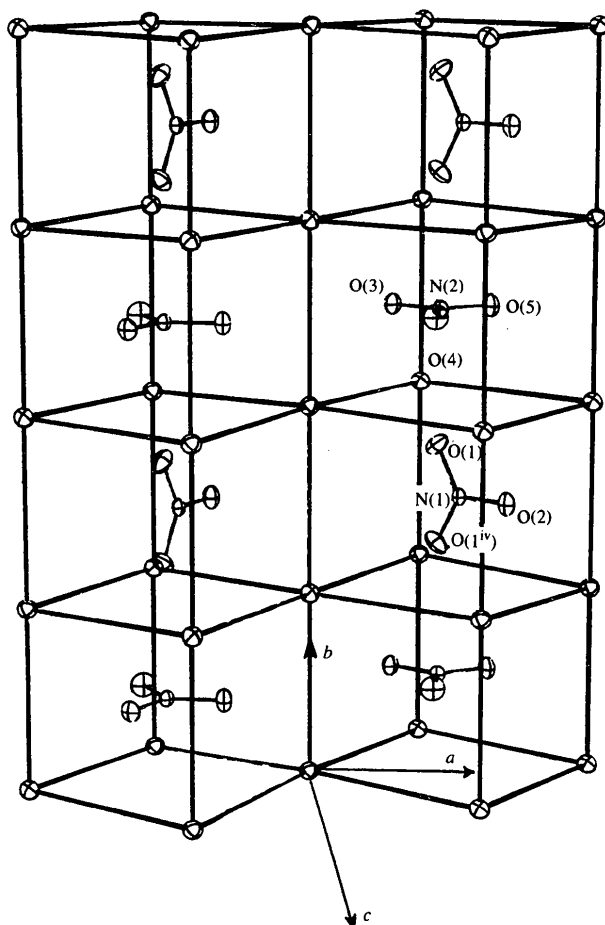


Fig. 1. An ORTEP drawing (Johnson, 1965) of the structure of TlNO_3 (III) showing the nitrate ions enclosed within the pseudo-cubic Tl subcells. The orthorhombic a and c axes are directed along the base diagonals of the pseudo-cubes as indicated. Displacement ellipsoids are shown at the 50% probability level.

with one of the N—O bonds parallel to another edge. The angles between the normals to the planes through the nitrate groups and the respective cube diagonals range from 55 to 58° .

The differences between the parameters obtained from the two studies are more prominent for the displacement parameters. Corresponding equivalent displacement parameters derived from the neutron study are more accurate and systematically lower than those derived from the X-ray study (Table 3). Mean square amplitudes of thermal motion for the two nitrate groups [$\text{N}(1)\text{O}_3$ and $\text{N}(2)\text{O}_3$] were estimated from the anisotropic displacement parameters using rigid-body vibration analysis (Cruickshank, 1956a). The principal r.m.s. amplitudes of translational motion range from 0.11 to 0.21 Å, and are almost comparable to the distortion of the cubes formed by the Tl ions. The principal r.m.s. amplitudes of librational motion (ω) vary from 6 to 8.8° ,

as shown in Table 5. The frequencies corresponding to these librations were computed using the method of Cruickshank (1956b). In a Raman spectroscopic study of the orthorhombic phase of TlNO_3 (Somayazulu, Roy & Deb, 1993) two prominent librational bands of the nitrate groups were observed, one at 145 cm^{-1} and the other at 120 cm^{-1} . However, these values were not assigned specifically to any one of the nitrate-group librations. Our thermal-vibration analysis (Table 5) shows that the frequencies of 134 cm^{-1} for $\text{N}(1)\text{O}_3$ (about the principal axis, which is nearly parallel to the crystallographic b axis) and 122 cm^{-1} for $\text{N}(2)\text{O}_3$ (with the principal axis parallel to the c axis) are the closest to the values observed by Raman spectroscopy.

Experimental

Single crystals of TlNO_3 were grown by slowly cooling an aqueous solution of TlNO_3 from high temperature using urea as a growth modifier, as reported earlier (Somayazulu, Sastry & Wadhawan, 1988).

Crystal data

TlNO_3
 $M_r = 266.38$
 Orthorhombic
Pnma
 $a = 12.355$ (5) Å
 $b = 8.025$ (3) Å
 $c = 6.298$ (2) Å
 $V = 624.4$ (4) Å³
 $Z = 8$
 $D_x = 5.679\text{ Mg m}^{-3}$

Neutron radiation
 $\lambda = 1.216$ Å
 Cell parameters from 50 reflections
 $\theta = 7\text{--}29^\circ$
 $\mu = 0.0068\text{ mm}^{-1}$
 $T = 300\text{ K}$
 Rhombohedral platelet
 $5.4 \times 3.8 \times 2.3\text{ mm}$
 White

Data collection

Four-circle diffractometer
 $\theta\text{--}2\theta$ step scans
 Absorption correction:
 by integration from crystal shape
 $T_{\min} = 0.983$, $T_{\max} = 0.987$
 230 measured reflections
 230 independent reflections
 191 observed reflections
 $[F_o^2 > \sigma(F_o^2)]$

$\theta_{\max} = 31.5^\circ$
 $h = 0 \rightarrow 10$
 $k = 0 \rightarrow 6$
 $l = 0 \rightarrow 5$
 2 standard reflections monitored every 50 reflections
 intensity variation: $<1\%$

Refinement

Refinement on F^2
 $R(F) = 0.0165$
 $wR(F^2) = 0.039$
 $S = 1.473$
 191 reflections
 61 parameters
 $w = 1/[0.03F_c^2 + 0.0076yk^2]^2$
 where $k = 4.857$ and y is the extinction coefficient

$(\Delta/\sigma)_{\max} = 0.06$
 Extinction correction:
 type II (Coppens & Hamilton, 1970)
 Extinction coefficient:
 $y_s(\min) = 0.12$
 Atomic scattering factors from *International Tables for X-ray Crystallography* (1974, Vol. IV)

Table 1. Fractional atomic coordinates obtained by neutron diffraction (this work)

	x	y	z
Ti	0.1244 (1)	0.5038 (1)	0.2142 (2)
N(1)	0.3897 (2)	1/4	0.2396 (3)
N(2)	0.3616 (2)	3/4	0.1645 (4)
O(1)	0.3569 (2)	0.1156 (3)	0.1690 (4)
O(2)	0.4577 (2)	1/4	0.3869 (4)
O(3)	0.2906 (2)	3/4	0.0221 (4)
O(4)	0.3324 (3)	3/4	0.3523 (8)
O(5)	0.4586 (2)	3/4	0.1126 (5)

Table 2. Differences between the fractional atomic coordinates for TiNO₃ (III) obtained by neutron diffraction (this work) and by X-ray diffraction (Fraser, Kennedy & Snow, 1975)

The pooled errors given in parentheses are dominated by the errors of the X-ray data.

	Δx	Δy	Δz
Ti	0.0000 (1)	-0.0001 (1)	0.0000 (2)
N(1)	0.0014 (21)	-	-0.0008 (36)
N(2)	0.0023 (18)	-	0.0017 (42)
O(1)	-0.0007 (17)	-0.0009 (25)	-0.0013 (34)
O(2)	-0.0030 (23)	-	-0.0015 (46)
O(3)	0.0009 (24)	-	0.0012 (47)
O(4)	-0.0012 (29)	-	0.0027 (46)
O(5)	-0.0002 (22)	-	-0.0024 (54)

Table 3. Equivalent isotropic displacement parameters (\AA^2) for TiNO₃ (III) from neutron diffraction (this work) and X-ray diffraction (Fraser, Kennedy & Snow, 1975)

	$B_{\text{eq}} = (4/3)\sum_i \sum_j \beta_{ij} a_i \cdot a_j$	
	Neutron study	X-ray study
Ti	2.76 (8)	2.96 (3)
N(1)	1.63 (9)	1.77 (61)
N(2)	1.64 (8)	1.65 (59)
O(1)	3.71 (10)	4.01 (57)
O(2)	2.89 (8)	3.49 (72)
O(3)	2.61 (10)	3.66 (76)
O(4)	3.70 (12)	4.57 (88)
O(5)	3.33 (10)	3.93 (79)

Table 4. Selected geometric parameters (\AA , $^\circ$) from the neutron diffraction study (this work)

Ti—O(2 ⁱ)	2.966 (2)	N(2)—O(4)	1.237 (5)
Ti—O(3 ⁱⁱ)	3.002 (2)	N(2)—O(5)	1.242 (4)
Ti—O(1 ⁱⁱⁱ)	3.010 (3)	N(2)—O(3)	1.254 (4)
Ti—O(2 ⁱⁱ)	3.030 (2)	Ti—O(3)	3.096 (2)
Ti—O(1 ^{iv})	3.041 (3)	Ti—O(4 ⁱⁱ)	3.103 (4)
Ti—O(5 ⁱ)	3.048 (2)	Ti—O(4)	3.356 (3)
N(1)—O(1)	1.235 (3)	Ti—O(5 ⁱⁱ)	3.390 (3)
N(1)—O(1 ^{iv})	1.235 (3)	Ti—O(1 ⁱ)	3.519 (3)
N(1)—O(2)	1.252 (3)	Ti—O(1 ⁱⁱⁱ)	3.556 (3)
O(1)—N(1)—O(1 ^{iv})	121.7 (3)	O(4)—N(2)—O(5)	122.2 (3)
O(1)—N(1)—O(2)	119.1 (1)	O(4)—N(2)—O(3)	118.7 (3)
O(1 ^{iv})—N(1)—O(2)	119.1 (1)	O(5)—N(2)—O(3)	119.1 (3)

Symmetry codes: (i) $\frac{1}{2} + x, \frac{1}{2} - y, \frac{1}{2} - z$; (ii) $\frac{1}{2} - x, -y, \frac{1}{2} + z$; (iii) $\frac{1}{2} - x, \frac{1}{2} + y, \frac{1}{2} + z$; (iv) $x, \frac{1}{2} - y, z$.

Table 5. Analysis of the librational motion of the nitrate groups in TiNO₃ (III)

Principal r.m.s. librational amplitudes ω ($^\circ$)	Moment of inertia $I \times 10^{40}$ (g cm^2)	Librational frequency ν (cm^{-1})	Direction cosines of principal axes with respect to the crystal axes			
			α_1	α_2	α_3	
N(1)O ₃	ω_1 6.01	61.3	134	0.09	0.99	-0.1
	ω_2 6.53	120.5	87	-0.66	0.16	0.73
	ω_3 7.90	62.6	100	0.74	-0.01	0.63

N(2)O ₃	ω_1 7.36	61.3	108	0.91	0.0	-0.41
	ω_2 8.78	123.3	64	0.0	1.0	0.0
	ω_3 6.51	62.2	122	0.0	0.0	1.0

A crystal was mounted with the b axis [the longer diagonal rhombohedral face (200)] along the φ axis of the four-circle neutron diffractometer (Rajagopal, Sastry, Shiv Bhaskar, Momin & Sequeira, 1993) at the DHRUVA reactor. Where the intensities of reflections could not be measured due to diffractometer geometry limitations, equivalent reflections were scanned. The data were reduced to structure factors using *DATRED* (Rajagopal, Srikanta & Sequeira, 1973, unpublished), which includes the absorption correction program *ORABS* (Wehe, Busing & Levy, 1962). The structural parameters, a scale factor (k) and anisotropic displacement parameters were refined on F^2 using the full-matrix least-squares program *TRXFLS* (Rajagopal & Sequeira, 1977, unpublished), a modified version of *ORFLS* (Busing, Martin & Levy, 1962). Initially a weighting scheme based on counting statistics was used where $w = 1/[\sigma_{\text{count}}^2 + (0.03F_o^2)^2]$. As the intensities were significantly affected by extinction, initial stages of refinement were carried out using an isotropic extinction correction of the form $y = (1 + 2x)^{-1/2}$ (Zachariasen, 1967) and omitting reflections strongly affected by extinction. In the final stages, a weighting scheme based on error analysis and an anisotropic extinction correction were introduced. A type II anisotropic extinction correction (Coppens & Hamilton, 1970) yielded better R values than a type I correction. Reflections with $F_o^2 < \sigma(F_o^2)$ and $|F_o^2 - F_c^2| > 4\sigma(F_o^2)$ were not included in the refinement. Refinements carried out using 170 reflections with $y > 0.4$ and using all 191 reflections yielded essentially the same parameters with no parameter varying by more than one e.s.d. The final anisotropic extinction parameters (in units of 10^6 mm^{-2}) were W_{11} 0.015 (2), W_{22} 0.018 (2), W_{33} 0.054 (6), W_{12} -0.006 (2), W_{13} -0.004 (3) and W_{23} -0.006 (2) where \mathbf{W} defines the anisotropic particle-size tensor, $r(\mathbf{N}) = [\mathbf{N}'\mathbf{W}\mathbf{N}]^{-1/2}$, \mathbf{N} being the unit vector normal to the incident beam and lying in the scattering plane.

We are grateful to Dr M. S. Somayazulu of the High Pressure Physics Division, BARC, for providing the single crystal.

Lists of structure factors, anisotropic displacement parameters and complete geometry have been deposited with the IUCr (Reference: BR1066). Copies may be obtained through The Managing Editor, International Union of Crystallography, 5 Abbey Square, Chester CH1 2HU, England.

References

- Brown, R. N. & McLaren, A. C. (1962). *Acta Cryst.* **15**, 977–978.
 Busing, W. R., Martin, K. O. & Levy, H. A. (1962). *ORFLS*. Report ORNL-TM-305. Oak Ridge National Laboratory, Tennessee, USA.
 Coppens, P. & Hamilton, W. C. (1970). *Acta Cryst.* **A26**, 71–83.
 Cruickshank, D. W. J. (1956a). *Acta Cryst.* **9**, 754–756.
 Cruickshank, D. W. J. (1956b). *Acta Cryst.* **9**, 1005–1009.
 Fraser, W. L., Kennedy, S. W. & Snow, M. R. (1975). *Acta Cryst.* **B31**, 365–370.
 Johnson, C. K. (1965). *ORTEP*. Report ORNL-3794. Oak Ridge National Laboratory, Tennessee, USA.
 Rajagopal, H., Sastry, P. U. M., Shiv Bhaskar, Momin, S. N. & Sequeira, A. (1993). XXIII National Seminar on Crystallography, I-1.

- Somayazulu, M. S., Roy, A. P. & Deb, S. K. (1993). *J. Phys. Condens. Matter*, **5**, 4557–4562.
- Somayazulu, M. S., Sastry, P. U. M. & Wadhawan, V. K. (1988). *Solid State Commun.* **67**, 757–761.
- Wehe, D. J., Busing, W. R. & Levy, H. A. (1962). *ORABS*. Report ORNL-TM-229. Oak Ridge National Laboratory, Tennessee, USA.
- Zachariasen, W. H. (1967). *Acta Cryst.* **23**, 558–564.

Acta Cryst. (1994). **C50**, 1857–1859

InBO₃

JAMES R. COX AND DOUGLAS A. KESZLER*

Department of Chemistry and Center for Advanced Materials Research, Oregon State University, Gilbert Hall 153, Corvallis, Oregon 97331 4003, USA

(Received 1 November 1993; accepted 13 April 1994)

Abstract

The crystal structure of indium borate, InBO₃, has been determined by single-crystal X-ray methods. The structure is similar to that of the mineral calcite, CaCO₃. Layers of distorted InO₆ octahedra are interleaved by layers of triangular-planar BO₃ units. The resulting indium-centered O octahedron exhibits a small trigonal elongation. The structure is compared and contrasted with other borates containing indium.

Comment

As part of a continuing effort to synthesize materials that possess promising optical properties, the compounds Sr₃In(BO₃)₃ and Ba₃In(BO₃)₃ were synthesized recently (Cox, Schaffers & Keszler, 1994). While attempting to delineate the crystal chemistry of these compounds and their relationships with the corresponding Sc derivatives, we discovered that the crystal structure of InBO₃ had not been refined. All references describing the structural characteristics of InBO₃ can ultimately be traced to the original X-ray work on powdered samples of materials isostructural with the mineral calcite, CaCO₃ (Goldschmidt & Hauptmann, 1932).

The unique optical properties exhibited by InBO₃ have resulted in several interesting applications. Tb³⁺-doped samples have been proposed for potential use as green cathode ray tube (CRT) phosphors in color televisions (Welker, 1991) and as real-time solar neutrino detectors (Chaminade *et al.*, 1990) on the basis of the inverse β -decay reaction $^{115}\text{In} \rightarrow ^{115}\text{Sn}^*$ (Raghavan, 1976). To characterize this material more completely, we report here its single-crystal structure refinement.

Single crystals were grown in a platinum crucible from a melt (Chaminade *et al.*, 1990) containing 3 g LiBO₂ (AESAR 99.9), 0.800 g In₂O₃ (AESAR 99.9) and 0.200 g B₂O₃ (Alpha 99.98). The melt was cooled from 1423 to 1113 K at 5 K h⁻¹ and then rapidly to room temperature. The flux was dissolved in hot distilled water to leave block-shaped crystals ranging in size from 0.2 to 0.8 mm. A suitable crystal was mounted on a glass fiber for data collection.

InBO₃ is isostructural with the mineral calcite, CaCO₃, as was predicted from X-ray powder diffraction photographs (Goldschmidt & Hauptmann, 1932). The present X-ray analysis verifies this prediction and also provides data on refined metrical parameters. In general, the structure is composed of alternating layers of In atoms and triangular planar BO₃ units as can be seen from the ball-and-stick representation of the unit cell (Fig. 1), with the In atoms occupying distorted octahedral sites. A similar type of layered structural coale-

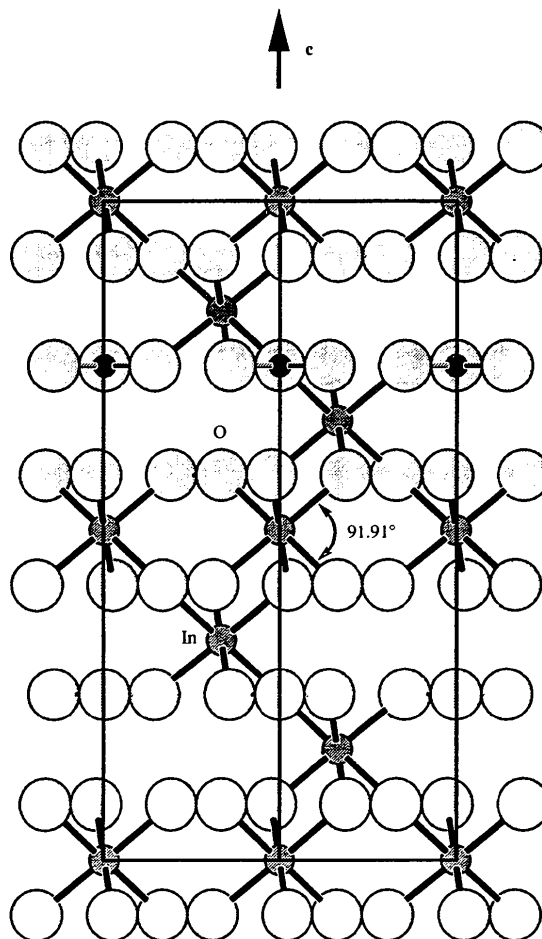


Fig. 1. Ball-and-stick representation of the InBO₃ unit cell with a [110] orientation. Filled black circles depict B atoms, medium shaded circles with dark bonds depict In atoms and the largest circles represent O atoms. This diagram also illustrates the elongation experienced by the InO₆ octahedra.